Reinsch, T., Henninges, J., Asmundsson, R. (2013): Thermal, mechanical and chemical influences on the performance of optical fibres for distributed temperature sensing in a hot geothermal well. - *Environmental Earth Sciences*, *70*, 8, 3465-3480,

DOI: 10.1007/s12665-013-2248-8

Environmental Earth Sciences manuscript No.
(will be inserted by the editor)

Thermal, mechanical and chemical influences on the performance of optical fibres for distributed temperature sensing in a hot geothermal well

Thomas Reinsch · Jan Henninges · Ragnar Ásmundsson

Received: 8 August 2012 / Accepted: 12 January 2013

Abstract Structural wellbore integrity is an important issue for a sustainable provision of geothermal energy. Raman scattering based fiber optic distributed temperature sensing (DTS) can help to monitor the status of a well and therefore help to optimize expensive work-over activities. This study reports on the installation of a fibre optic cable in the cemented annulus behind the anchor casing in the high temperature geothermal well HE-53, Hellisheiði geothermal field, SW Iceland. Although the cable has been damaged during the installation, temperature data could be acquired during the entire length of installation down to 261.3 m. Temperature measurements were performed during the installation in spring 2009, during the onset of a flow test in summer 2009 and after a 8.5 month shut-in period in summer 2010. During the flow test, maximum temperatures of 230 °C were measured after two weeks fluid production. Using optical time domain reflectometry (OTDR), attenuation measurements at 850 and 1300 nm enabled to identify mechanical, thermal, and chemical degradation along the optical fibre. The observed degradation led to erroneous temperature readings and limits, due to the optical budget of the DTS system, the accessible length of the fibre. The characteristics and the influence of the different degradation mechanisms on the accuracy of the DTS measurements are discussed and recommendations for an optimized installation are given.

Thomas Reinsch
Helmholtz Centre Potsdam, GFZ German Research Centre for Geosciences, Telegrafenberg, 14473 Potsdam, Germany
Tel.: +49-331-2881834
Fax: +49-331-2881450
E-mail: Thomas.Reinsch@gfz-potsdam.de

Jan Henninges
Helmholtz Centre Potsdam GFZ German Research Centre for Geosciences, Telegrafenberg, 14473 Potsdam, Germany

Ragnar Ásmundsson
Heat Research and Development, Varmalausnir, Akureyri, Iceland

Keywords distributed temperature sensing (DTS) · Iceland · high temperature geothermal well · optical fibre · optical time domain reflectometry (OTDR)

PACS 93.30.Ge · 93.85.Fg · 07.20.Dt · 42.81.Cn · 07.60.Hv · 88.10.gk

1 Introduction

Within mitigation strategies for the climate change, geothermal energy plays an important role for the future energy supply (Sims et al, 2007). In order to characterize a geothermal reservoir and to design a strategy for a sustainable production of energy, measuring transient well-bore temperatures is important. It is well established that transient temperature measurements after the drilling process can be used to determine static formation temperatures (e.g. Dowdle and Cobb, 1975). Furthermore, they can also be used to identify relevant feed zones to a well (e.g. Nowak, 1953; Stefánsson and Steingrímsson, 1980). Formation temperatures as well as temperature changes during the production or injection of geothermal fluid are necessary informations to design the infrastructure at a geothermal site (e.g. Saadat et al, 2010).

Over the last two decades, fibre optic distributed temperature sensing (DTS) based on Raman backscattering has been increasingly used for wellbore applications, e.g. in the petroleum industry (Williams et al, 2000; Johnson et al, 2004; Pimenov et al, 2005) as well as for geothermal (Hurtig et al, 1994; Förster et al, 1997; Günzel and Wilhelm, 2000; Henninges, 2005) and climate studies (Freifeld et al, 2008). Apart from wellbore applications, DTS systems have been applied for pipeline leak detection (e.g. Tanimola and Hill, 2009) or underground mine surveillance (e.g. Aminossadati et al, 2010). DTS-technology is a means to acquire quasi continuous temperature measurements along the entire length of an optical fibre. Integrating an optical fibre in an appropriate wellbore cable, a temperature profile over the entire length of the cable can be determined. Permanently installed behind casing, temperature information can be acquired without well intervention.

DTS is especially well suited for the application under harsh well-bore conditions. The passive fibre optic cable can be remotely controlled and no electronics have to be lowered into the well. To acquire a continuous temperature profile, a laser pulse is coupled into the fibre and backscattered photons of the Stokes and Anti-Stokes wavelengths are recorded. The ratio of these signals can be calibrated to ambient temperatures and is therefore sensitive to differential attenuation changes within these frequency bands along the fibre. From the travel time of the signal, the location of the temperature information along the fibre can be determined (e.g. Hartog, 1983).

Conventional high temperature geothermal wells, like in high enthalpy areas in Iceland, reach temperatures up to $350 - 380\,^{\circ}\mathrm{C}$ (Arnórsson, 1995). To increase the energy output from individual geothermal wells, accessing unconventional geothermal reservoirs comes into the focus of current research

activities (e.g. Fridleifsson and Elders, 2005; Bignall, 2010). Tapping geothermal fluids at supercritical conditions might enhance the energy output from a single well by an order of magnitude (Albertsson et al, 2003). In order to acquire temperature data from such wells, electronic as well as fibre optic logging devices can be used.

Although special optical fibres have to be selected for the application in a hot geothermal well, optical fibres are well suited for the application at elevated temperatures. Beside temperature, the ingression of hydrogen is an important aspect that has to be considered using optical fibres in harsh environments. Within the geothermal fluid of high temperature geothermal wells in Iceland, hydrogen is often present (Arnórsson, 1995). In the presence of hydrogen, however, optical properties of fibres degrade rapidly due to hydrogen ingression and hydroxyl formation (Smithpeter et al, 1999; Williams et al, 2000; Normann et al, 2001).

The ingression of hydrogen and the subsequent formation of hydroxyl causes strong absorption peaks at relevant wavelengths (Stone and Walrafen, 1982; Humbach et al, 1996; Williams et al, 2000). The increasing absorption at individual wavelengths leads to an increase in the differential attenuation between the Stokes and Anti-Stokes band. Changing the differential attenuation skews temperature measurements over time, i.e. measured DTS temperatures become increasingly different to ambient temperature conditions (Normann et al, 2001). The ingression of hydrogen in to the fibre can be reduced using hydrogen diffusion barriers like hermetic carbon coatings. Although carbon acts as a hydrogen diffusion barrier at low temperatures, hydrogen diffusion can be detected at temperatures above 100 °C (Lemaire and Lindholm, 2007). Pure silica core fibres have been shown to be an alternative for application in hydrogen rich environments (Kaura and Sierra, 2008).

Mechanical stress onto the fibre can lead to micro- and macrobending loss, influencing the wavelength dependent attenuation characteristics. Changing temperatures, a different coefficient of thermal expansion (CTE) between coating and silica material as well as thermal degradation and stiffening of coating material can cause *microbending* loss, which is defined as the loss induced by "'small random bends and stress in the fibre axis"' (Lingle, Jr. et al, 2007). Large deflections of the fibre axis, i.e. caused by localized mechanical stress onto the cable, leads to *macrobending* loss.

In order to monitor wavelength dependent transmission changes along the fibre, attenuation measurements at standard telecommunication (850 and 1300 nm) wavelengths can be used to qualitatively monitor the optical properties (Smithpeter et al, 1999). Hydrogen ingression,causes strong absorption peaks which can be detected using the attenuation ratio $\frac{a^{1300}}{a^{850}}$ (Humbach et al, 1996; Smithpeter et al, 1999). Due to the proximity of the 1300 nm testing wavelength to the hydroxyl absorption peaks at 1270 and 1380 nm, the ratio increases with increasing hydrogen load of the optical fibre. Using the ratio of attenuation values, different degradation processes and resulting influences on the measured temperatures can be assigned to different regions along the fibre.

In order to reduce the influence of a differential attenuation change along the fibre, conventional DTS systems allow for measurements from both sides of the fibre. If there is no possibility for temperature reference points along the fibre, averaging measurements from both ends of the fibre can be used to correct for a differential attenuation change and hence a measured temperature change (van de Giesen et al, 2012). Beside these so called double-ended measurementsLee (2007); Suh and Lee (2008) presented the dual laser principle to reduce the effect of hydrogen on the measured temperature. Here, measurements from two different incident wavelengths are used to correct for hydrogen absorption. The dual laser principle can be used to detect differential attenuation changes if only one end of the fibre can be accessed. Furthermore, recent DTS systems allow for self-inspection and self-calibration during the temperature measurement.

This study was designed to test the performance of a novel fibre optic cable under in-situ conditions. Within an earlier study (Reinsch and Henninges, 2010), a polyimide-coated graded-index multimode fibre with an additional hermetic carbon layer between coating and cladding has been chosen for deployment. Using this fibre type, a novel fibre optic cable has been developed, manufactured, tested prior to the installation (Reinsch, 2012) . Here, we report on the installation of the fibre optic cable behind the anchor casing of well HE-53 in the Hellisheiði geothermal field in SW Iceland as well as the performance of the cable during three different field campaigns. Temperature and attenuation measurements were performed during the cementation (May 2009) of the anchor casing and the onset of a flow test (July/August 2009) as well as after the termination of this flow test when wellbore temperatures reached static formation temperatures, again (August 2010).

Details on the calibration procedure as well as the measured field data can be accessed in a supplementary data publication (Reinsch and Henninges, 2012).

1.1 Hellisheiði Geothermal Field

The Hellisheiði geothermal field is situated in SW Iceland, close to the Hengill central volcano. The Hengill volcanic system is associated with two presently exploited geothermal systems. To the North, the Nesjavellir geothermal field is used to produce electrical energy and hot water for space heating since several years. Recently, the Hellisheiði geothermal field in the south of the volcano was started to be exploited. Due to the meteoric origin of the geothermal fluid in the Hengill area (Arnórsson, 1995), the salinity in Hellisheiði is very low with a concentration of total dissolved solids of approx. 1500 ppm (Franzson et al, 2005).

Within the Hellisheiði area, HE-53 is situated in the Hverahlíð geothermal field. The geology in the vicinity of well HE-53 is dominated by lava successions with intercalated hyaloclastite formations, formed in underwater eruptions. Rock alterations caused by geothermal activity range from fresh rocks which

are in contact to the shallow groundwater aquifers through zeolith assemblages to high temperature assemblages. In between the volcanic succession, intrusive rocks can be found (Níelsson and Franzson, 2010).

From deep wells (2000-2800 m) it is known that a high temperature system of $200 - 320$ °C is situated below $600 - 1000$ m depth (Níelsson and Franzson, 2010). Geothermal fluid within the Hellisheiði geothermal field is currently produced from 30 wells which are operated at wellhead pressures from $15 - 25$ bar (Sigfusson and Gunnarsson, 2011). As the produced fluid is at the boiling point, temperatures can be derived from steam tables. Pressures of $15 - 25$ bar at the wellhead, therefore, correspond to temperatures of $200 - 225$ °C (Lemmon et al, 2007). The wells have an average discharge of 37 kg/s and an enthalpy of 1675 J/kg (Sigfusson and Gunnarsson, 2011).

2 Installation of DTS Sensor cable

2.1 Concept

The novel wellbore cable has been developed in collaboration with nkt cables GmbH (Geckeis et al, 2011). Its outer diameter (OD) is 5.0 ± 0.2 mm. The sensing fibre is embedded in a stainless steel (material 1.4301) loose tube with an outer diameter of 1.8 mm. The armour is made of bronze wire. Water blocking yarn is used to reduce fluid migration along the cable. A second stainless steel loose tube (OD 3.5 mm) protects the armour. The cable is jacketed with a 0.75 mm layer of perfluoroalkoxy (PFA).

In Iceland, the casing profile of high-temperature geothermal wells is standardized following the standard American Petroleum Institute (API) oilfield tubular diameters (Thorhallsson, 2008). A typical casing profile for high-temperature wells, which is used in the Hellisheiði geothermal field as well, is shown in Figure 1(a). Based on the expected flowrate of less than 80 kg/s, a "slim hole" casing diameter with a 9 5/8" production casing has been chosen for well HE-53 (Table 1).

In order to avoid an additional feed-through for the cable at the wellhead, it has been installed behind the anchor casing. For the installation of the anchor casing, conventional rigid blade centralizers are used (Econ-o-glider^{TM}, Downhole Products Ltd., OD 17"). The cable is attached to the centralizers, using button head ties. In between the joints, tape and cable ties are used to attach the cable close to the casing. On the joints, the cable is attached with tape, again. Thus, the distance between anchor casing and cable varies along the well between zero and approx. three centimetres, respectively (Figure 1(c)). A centralizer is installed underneath every joint below the surface casing and underneath every second joint within the surface casing.

In order to increase the lifetime of the cable and the accuracy of the measurements, an installation in a loop configuration with a 180° separation between both cable branches around the perimeter of the casing was chosen. The loop configuration was designed to allow for performing DTS temperature mea-

Table 1 Diameter of drill bit and casing as well as depth information for well HE-53 (Icelandic nomenclature and drillers depth; courtesy of Reykjavik Energy).

Casing	Bit Size (in)	Casing OD (in)	Drilling Depth (m)	Casing Depth (m)
Surface Casing	21	18 5/8	62.8	61.3
Anchor Casing	17 1/2	13 3/8	302.8	299
Production Casing	12 1/4	9 5/8	959.1	959
Perforated Liner	8 1/2	7	2500.6	2463.3

surements from both ends of the fibre and therefore reduce the detrimental effects of fibre alteration on the measured temperatures. The 180° separation of the cable was meant to increase the probability for a successful measurement of a temperature profile down to the total depth of installation. Damaging one branch of the cable, the probability for an undamaged second branch would be higher. DTS temperature measurements in single ended configuration would still be possible.

For the turnaround at the very bottom of the cable installation, two of the centralizers' rigid blades have been carved and additional aluminium profiles were attached to fix the cable (Figure 1(b)). In order to protect the cable during installation of the casing, a second centralizer was mounted to the casing below the modified one with an offset of 30°.

The loop configuration, furthermore, allows for a continuous flushing of the cable with Argon. It is known that heating the fibre in inert atmosphere instead of air is capable of reducing the degradation of the coating (Reinsch and Henninges, 2010). Furthermore, it has been observed that flushing the cable could significantly contribute to a reduction of harmful chemical species (e.g. hydrogen released from the cable itself due to cracking of forming oil at elevated temperatures Williams et al, 2000; Reinsch, 2012) along the cable and therefore increase the lifetime of the installation at high temperatures.

2.2 Field Work

The fibre optic cable has been installed down to a depth of 261.3 m. During the installation, the cable was accidentally cut two times, leaving one end accessible down to 179.5 m (western side of the well) and the second down to the turnaround at 261.3 m (eastern side of the well). Furthermore, a damage of the fibre at the eastern side was detected in a depth of about 235 m (Figure 5(a)). For the accessible parts of the cable, similar attenuation values were measured before and after the installation.

Having the cable cut, flushing it with Argon could not be performed. Potential harmful chemical species could not be removed from the cable. With the fibre only accessible from one end, DTS measurements could be performed in single-ended configuration. Furthermore, the state of the cable for each branch was monitored using optical reflectometry techniques, only.

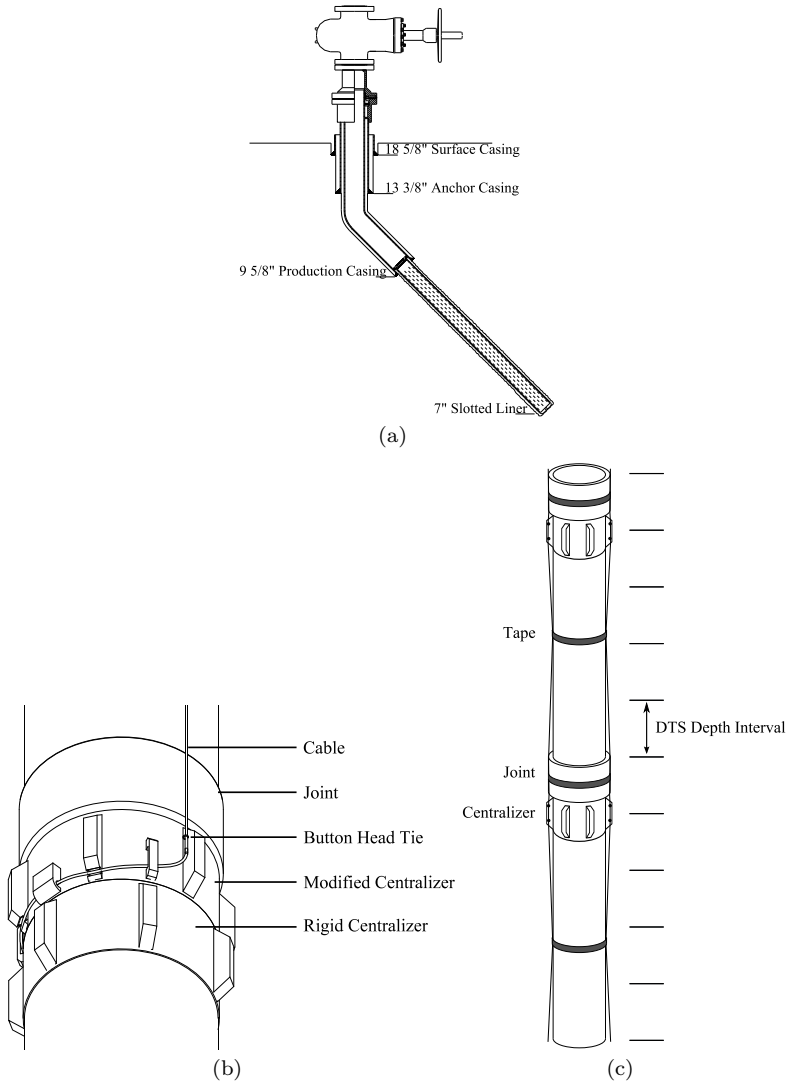

Fig. 1 (a) Casing profile for Icelandic high temperature wells (modified after Thorhallsson, 2003, Icelandic nomenclature) and (b) schematic sketch of the turnaround below the first casing joint above the float collar. (c) Sketch showing the position of the cable behind casing. DTS temperatures are averaged over a 1 m interval, which is indicated as well (not to scale).

3 Fibre Optic Measurements

Three successive field campaigns have been performed. First, data have been acquired directly after the installation of the sensor cable during the cementation of the anchor casing in May 2009. Data were used to evaluate the performance of the cementation as well as to test the measurement equipment after

installation. A second field campaign has been performed during the onset of a flow test in July/August 2009 to evaluate the performance of the fibre optic cable during rapid temperature changes and at high temperature conditions. In order to gather information about the state of degradation of the fibre-optic cable after the three-month flow test, a third campaign has been performed in August 2010 after a subsequent 8.5 month shut-in period.

Prior to the field campaign, the wellbore cable has been calibrated to the expected temperature range. In laboratory tests, the absolute temperature accuracy over the entire temperature range from $0 - 240$ °C has been determined to be 0.5 °C for an integration time of about 10 min (Reinsch and Henninges, 2012).

3.1 Experimental Set-Up and Measurement Schedule

For the three field campaigns, a similar experimental set-up was used (Figure 2). A 100 m fibre optic extension terminated with E2000 APC connectors was used to connect the surface readout unit (SRO) with the wellbore cable. Therefore, a pigtail terminated by an E2000 APC connector has been spliced to the wellbore cable. At the surface, an excess length (SEL $\geq$ 15 m) of the wellbore cable was accessible to gather reference temperature information (Table 2).

For the first measurement campaign, the SEL was placed on the rig and exposed to ambient weather conditions. Reference temperature information was gathered from the nearby weather station Hellisheiði to evaluate the absolute accuracy of the measurements. For the second and third campaign, the SEL was placed in an ice bath and a temperature offset correction was applied. Temperature data from the third campaign have been compared to an undisturbed temperature profile from shortly before the flow test and to a conventional temperature log which was measured simultaneously in the neighbouring well HE-36 (horizontal distance approx. 10 m). As DTS measurements were performed over a large temperature range, an additional polynomial temperature correction has been applied to the measured data. Further details can be found in Reinsch and Henninges (2012).

Distributed temperature measurements were conducted using a DTS800 from Sensa with a 1064 nm Nd:YAG-laser. Beside temperature measurements, optical time domain reflectometry (OTDR) measurements were performed to determine the optical attenuation at 850 and 1300 nm using a MTS5100 from Wavetek. The evolution of attenuation over time is used to evaluate the degradation of the optical fibre. As sensing fibre, a 50/125 μm graded-index multimode fibre was used (Geo50 fibre from OFS Fitel, LLC). The coating was made of polyimide with an additional carbon layer between clad and coating.

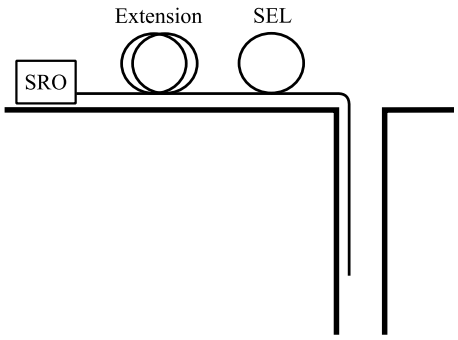

Fig. 2 Schematic experimental set-up for DTS and OTDR measurements. The surface readout unit (SRO) is connected via an optical extension to the surface excess length (SEL) of the wellbore cable.

Table 2 List of the three logging campaigns. The begin of the individual measurements is listed together with the duration of the campaign and the acquisition time for individual logs.

#	Begin DTS Measurement	Duration (h)	Acquisition Time (s)	SEL	Offset Correction
1	05/04/2009 00:25	46	27	ambient	no
2	07/28/2009 16:52	115	18	ice bath	yes
	since 08/02/2009 12:20	241	104	ice bath	yes
3	08/10/2010 15:54	25	103	ice bath	yes

3.2 Results

3.2.1 Temperature Measurements

First DTS Logging Campaign: Cementation The temperature evolution within the annulus during the cementation of the anchor casing is shown in Figure 3 (left). Temperature within the annulus is generally increasing during the measurement. Periodic temperature variations can be seen with depth. The wavelength is approximately $5-6$ m. For the first few hours, temperature stays constant with variations below 5 °C (profiles at 3 and 5 h). After that, temperature increases rapidly by more than 40 °C (profiles at 20 and 25 h). A strong temperature decrease and a smoothing of the temperature profile was observed between 25 and 40 h for the uppermost 107 m. The temperature decrease corresponds to the time when the casing has been filled with cold water for cement bond logging (CBL) at about 29.5 h_{DTS}.

Second DTS Logging Campaign: Flow Test For the flow testing period, temperature data for different times are shown in Figure 3 (middle). Prior to production testing in well HE-53, baseline temperature measurements were

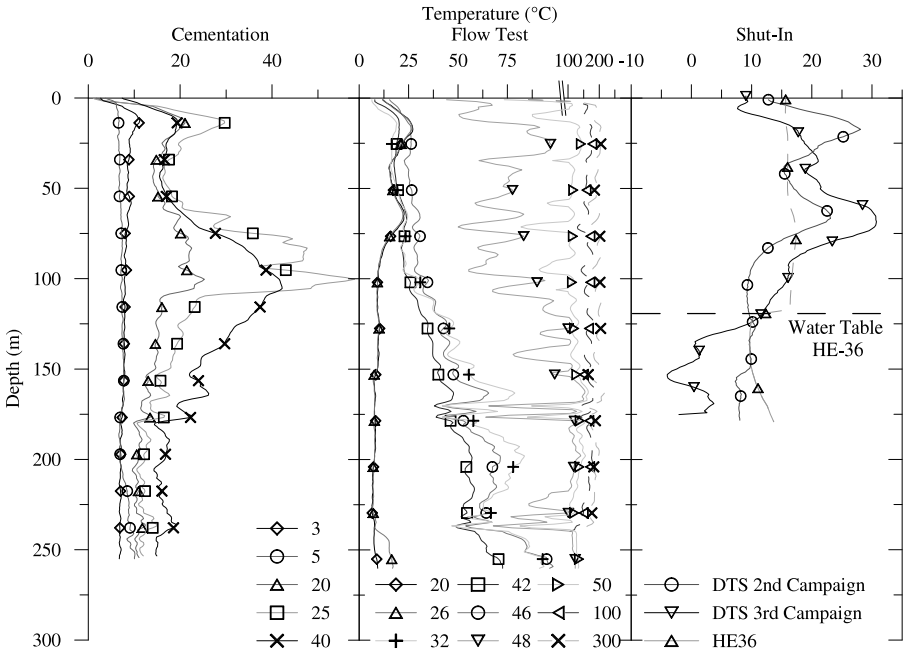

Fig. 3 DTS Temperature profiles recorded at different times (h) after beginning of logging during the three different field campaigns (3 m moving average). Left: cementation (27 s temporal average), middle: flow test (18 s temporal average before and 104 s after 115 h_{DTS}) and right: shut-in (1 h temporal average). For the shut-in, additional temperature data from well HE-36 is given together with the water table in this well. Data from HE-36 courtesy of Reykjavik Energy.

performed ($0 - 20$ h_{DTS}[1]). The temperature profile was almost homogeneous at about 10 °C along the cable, except for two variations in $0 - 37$ m and $39 - 78$ m, where measured temperatures were considerably higher by 10-15 °C (profile at 20 h_{DTS}). Temperature variations with time were not observed. As the measurement was performed one month after well completion, the well temperature is assumed to be rather close to the undisturbed formation temperature.

After 20 h of logging, the well was opened for bleeding, i.e. gas at top of the well column was released. During the first 6 h of bleeding, temperatures below approx. 235 m increased by about 10 °C (profile at 26 h_{DTS}). The temperature profile above did not change. Afterwards, a subsequent temperature increase was observed in subsequently shallower depth intervals. Starting at the bottom of the installation, the temperature increase continued to migrate upwards (profile at 32 h_{DTS}). Temperatures below 40 m increased whereas they decreased above. Initially high temperatures of 25 °C in 15 m depth, for example, decreased by 8 °C. At about $30 - 32$ h_{DTS} the temperature profile

[1] For the second logging campaign, the beginning of the DTS logging is used as reference time; h_{DTS}

stabilized. The temperature increase below 70 m slowed down and temperatures even decreased, again. A rapid increase was observed after 46 h, when the well was opened for production (profile at 46 h_{DTS}). For the entire time DTS measurements were performed, increasing temperatures were measured afterwards. Shortly after the rapid temperature increase, the DTS signal was lost below 235 m. The measurements were stopped after two weeks of continuous logging.

The overall temperature signal exhibits similar periodic changes with depth as observed during the cementation. Furthermore, strong negative temperature excursions were measured in about 175 m and 235 m. Maximum temperatures measured within the annulus at the end of the measurement campaign reached 229.98 °C at 162.87 m (Figure 4). At specific times, e.g. at time 173.3 h_{DTS}, strong temperature variations were observed along the entire temperature profile (Figure 4). These times correspond to the time of OTDR measurements, when the connectors have been switched between the different surface readout units.

After the end of the fibre optic logging campaign, flow testing continued until end of November 2009. Figure 4 shows the calculated evolution of the wellhead temperature in comparison to the measured DTS temperature. After starting the measurement at 68 h_{DTS}, wellhead pressure was continuously measured during the production period. As a two phase fluid is produced from the well, the wellhead temperature has been calculated according to the boiling point curve of pure water (Lemmon et al, 2007). The wellbore fluid salinity in the Hellisheiði geothermal field is below 1500 ppm (Franzson et al, 2005). Calculated temperatures are therefore slightly lower than actual values. The difference, however, is small (less than 0.5 °C at 100 °C and 1 bar for 1500 ppm NaCl, Driesner and Heinrich, 2007) and therefore neglected in the following.

Third DTS Logging Campaign: Shut-In The measured DTS temperature during the third logging campaign is shown in Figure 3 (right) together with a conventional temperature profile simultaneously acquired in the neighbouring well HE-36 and a temperature profile from the beginning of the second field campaign. After the end of the flow test, temperature data could be recovered down to a depth of 175 m. Below, the signal was lost. Two temperature maxima could be observed within the uppermost 90 m, with a minimum in about 40 m depth. Below, the temperature decreases to approx −4 °C in a depth of 155 m. Further down, temperatures increased slightly, but remained below 5 °C.

The DTS temperature from the beginning of the second field campaign is shown in comparison. It is assumed to resemble undisturbed formation temperatures, as mentioned above. Temperature data between both measurements differ by more than 10 °C in specific depth intervals. Although DTS temperature from after the flow test is about 10 °C higher than before in the depth interval $40 - 120$ m, the overall appearance with two maximum temperatures and a minimum in between in a depth of about 40 m is similar. Below, temperature data are much lower after the flow test, compared with data acquired

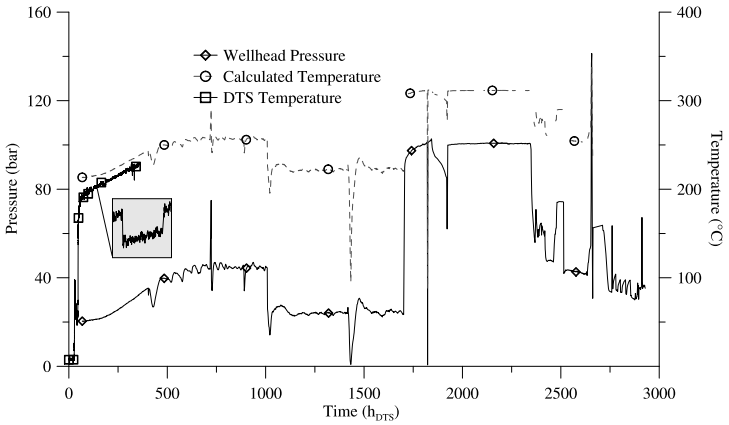

Fig. 4 Comparison of wellhead temperature evolution and DTS temperature readings during a flow test in HE-53 in 2009. Temperatures at the wellhead are calculated according to the boiling point pressure for pure water. DTS temperature readings from a depth of 162.87 m below ground surface are displayed. The inset plot shows a zoom in for the period $170 - 190$ h_{DTS}. Wellhead pressure courtesy of Reykjavik Energy.

before. Furthermore, strong variations, as observed after the flow test, were not measured before.

The temperature profile in well HE-36 differs from the DTS profiles, as it has been acquired using a conventional slickline temperature gauge. Above the water table, therefore, the temperature profile is almost homogeneous at about 16 °C. Below, the profile is almost homogeneous for approx. 35 m ($120 - 155$ m) at about 10 °C. Further down, the temperature in HE-36 increases slowly. For the depth interval $120 - 155$ m, temperature readings for the beginning of the second logging campaign and the profile measured in HE-36 are similar. Above and below, they are different.

3.2.2 Attenuation Measurements

First DTS Logging Campaign: Cementation Attenuation measurements from before the installation and after cementation are shown in Figure 5(a). Before the installation, the attenuation profile was smooth, showing no signs of damages along the cable. During the installation, the cable was accidentally cut two times. A further damage could be detected on the longer branch on the eastern side (Section 2.2). Changes of the attenuation during the cementation were not detected.

Second DTS Logging Campaign: Flow Test During the second logging campaign, OTDR attenuation measurements were performed two times a day. Attenuation profiles from the beginning and the end of the second logging campaign are shown in Figure 5(a) (profiles 0 and 356 h_{DTS}). According to the attenuation profile at 356 h_{DTS}, different regions have been assigned along the fibre. Region 1 ($0 - 170$ m) is the uppermost region with a relatively smooth

attenuation profile. Region 2 ($170 - 180$ m) is characterized according to the sharp attenuation increase which evolves in the course of the test in comparison the profile acquired at 0 h_{DTS}. The third region ($180 - 230$ m) is again characterized by a smooth attenuation profile and terminated by the damage in about 235 m, detected during the installation. This damage and the part of the fibre lost during the flow test ($230 - 261$ m) belongs to region 4. During heating of the well, changing attenuation ratio values were detected in different sections along the fibre (Figure 6(a)).

1. **Region 1**: No changes of the attenuation ratio could be detected in this region. The attenuation at 850 nm, averaged over the interval $0 - 150$ m, remained similar from 2.3 dB/km after the installation to 2.4 dB/km at the beginning of the flow test but increased to 2.7 dB/km at the end of the second logging campaign. During the high temperature period, the attenuation at 850 nm continuously increased, as shown in Figure 6(b).
2. **Region 2**: The attenuation ratio changes significantly in the course of the experiment. It increases rapidly with increasing temperature (Figure 6(a)).
3. **Region 3**: A small linear increase of the attenuation ratio was detected over time. The attenuation at 850 nm almost doubled to 4.2 dB/km for this region (averaged over the interval $190 - 220$ m).
4. **Region 4**: After heating of the well, no data could be collected below approx. 230 m.

Third DTS Logging Campaign: Shut-In After the flow test, data could only be acquired for region 1 (Figure 5(a), profile at 9047 h_{DTS}). The fibre was cut in region 2 in about 175 m, where the damage was detected during the onset of the flow test. The attenuation at 850 nm increased from 2.4 dB/km at the beginning of the flow test to 18.6 dB/km at the time of the third logging campaign. Differential attenuation along the fibre increased by approx 100 % (Figure 6(a)).

In Figure 5(b), the attenuation has been plotted without the trend shown in Figure 5(a). The attenuation change strongly corresponds to the temperature profile which was measured during the flow test. High attenuation values correspond to sections of high temperature along the fibre.

3.2.3 Accuracy

In order to estimate the accuracy of the DTS measurement during the three field campaigns, different error sources have been evaluated and an attempt has been made to give approximate values for these errors. A strong influence on the measured DTS temperature has been observed during un-plugging and re-plugging of the DTS connectors for OTDR measurements (ΔT_{con}). Furthermore, elevated temperatures can have an influence on the measured DTS temperature due to a degradation of the optical fibre ΔT_{deg}.

For double ended measurements using the experimental set-up described in Reinsch and Henninges (2012), the absolute accuracy for the temperatures

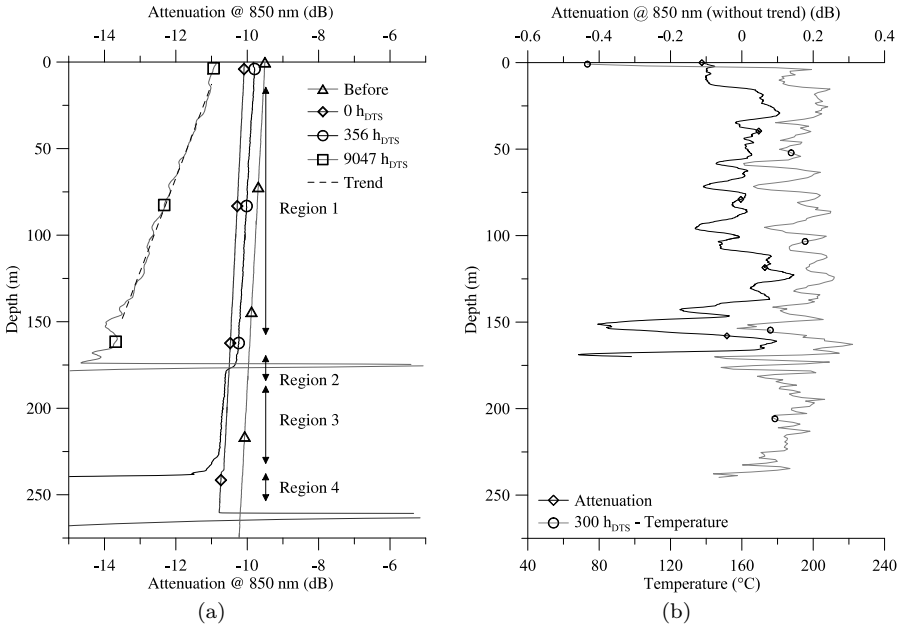

Fig. 5 Attenuation profiles at 850 nm (a) before installation and for the second (0 and 356 h_{DTS}) and third (9047 h_{DTS}) measurement campaign. The profile recorded at the end of the first logging campaign is similar to the profile recorded at 0 h_{DTS} at the beginning of the second logging campaign and is therefore not displayed. Different regions along the fibre are indicated (see text for details). (b) Attenuation at 9047 h_{DTS} without trend shown in (a), in comparison to a temperature measurement from during the flow test.

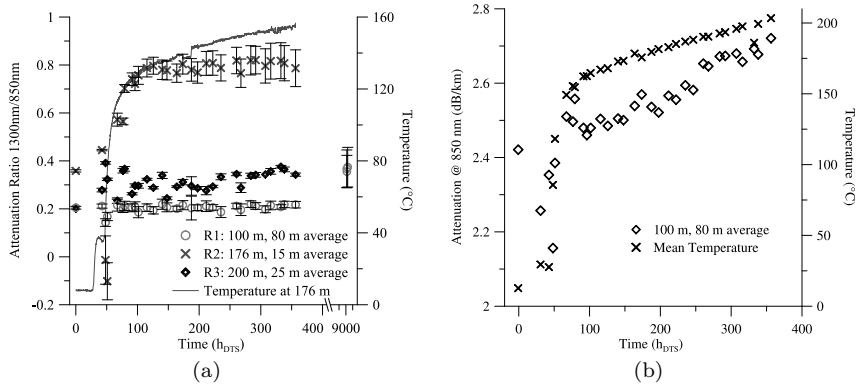

Fig. 6 (a) Attenuation ratios for the different regions (R1-R3) of the eastern cable branch during the flow test. Values measured during the third campaign are displayed for region 1, as well. (b) Average attenuation at 850 nm together with the mean DTS temperature within region 1.

Table 3 Estimated DTS temperature error values associated with the three measurement campaigns (ΔT_{DTS}). Except for the first campaign, the offset recorded at the SLE has been corrected. DTS measurements have been suspended for OTDR measurements during the second field campaign, only. The error associated with the connector change (ΔT_{con}), therefore is neglected for the other campaigns. For further details, see text.

Error (°C)	Cementation	Flow Test	Shut-In
ΔT_{off}	1.3	0.0	0.0
ΔT_{con}	0.0	2.0	0.0
ΔT_{cal}	0.5	0.5	0.5
ΔT_{rel}	0.1	0.1	0.1
ΔT_{deg}	0.0	0.0	>10
ΔT_{DTS}	1.9	2.6	>10

below 240 °C has been determined to be about ΔT_{cal} =0.5 °C (Reinsch and Henninges, 2012). The relative accuracy for the DTS800 expected for this measurement has been determined to be about ΔT_{rel} =0.1 °C for an integration time of 10 min in double ended configuration (Henninges et al, 2005b) for a fibre of 2908 m length. For single ended measurements, however, these values increase, as non-linear differential attenuation changes between the Stokes and Anti-Stokes signal cannot be compensated for and the initial linear differential loss between both bands has not been accurately determined for this cable. As only single ended measurements could be performed, a constant offset ΔT_{off} has been determined for the different measurement campaigns at the SLE. The combined error is therefore:

$$\Delta T_{DTS} = \Delta T_{off} + \Delta T_{con} + \Delta T_{cal} + \Delta T_{rel} + \Delta T_{deg} \quad (1)$$

Table 3 lists the estimated maximum measurement errors associated with the different field campaigns for region 1 of the eastern cable branch.

First DTS Logging Campaign: Cementation In order to quantify the absolute accuracy of the DTS measurements during the cementation process, the DTS temperatures along the SEL of the eastern cable branch were measured and compared to ambient weather conditions (Figure 7). On average, temperatures logged by the DTS were ΔT_{off} =1.3 °C lower than temperatures from the weather station with a standard deviation of 0.3 °C. Depending on the speed of the wind, which blew constantly roughly from the station in direction to the well, the difference ranged from 0.5 to 2.0 °C.

Second DTS Logging Campaign: Flow Test At high temperatures, bad connectors have a significant influence on the measured temperature due to an increase in differential attenuation of the backscattered signal. After correcting for the temperature loss in the ice bath, an influence on the temperature of up to ΔT_{con} =4.6 °C has been detected (Figure 4 at 173.3 h_{DTS}) for a damaged fibre optic extension. Changing the extension could significantly reduce the error at 187 h_{DTS}. At other times (e.g. 163 h_{DTS} or 198 h_{DTS}, Figure 6(a))

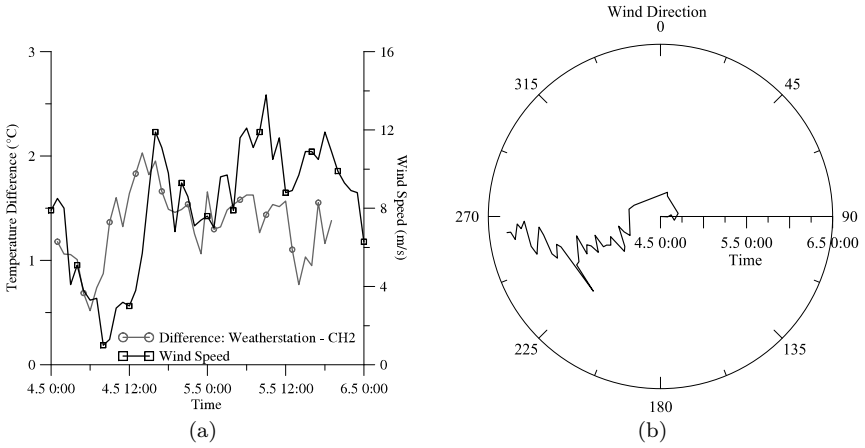

Fig. 7 (a) Average DTS temperature measurements along the surface excess length in comparison to data measured by a nearby weather station. (b) Wind direction during the measurement. Weather data courtesy of the Icelandic Meteorological Office, Station Hellisheiði (64°1.127', 21°0.543' (64.0188, 21.3424)).

the error introduced by plugging and unplugging resulted in a temperature change lower than ΔT_{con} =2.0 °C in the depth of 162.87 m, where maximum temperatures were measured in the course of the second field campaign (Figure 4).

Third DTS Logging Campaign: Shut-In From the comparison of different temperature profiles in Figure 3 (right), it can be seen that DTS temperature readings after the flow test differ by ±10 °C from temperatures measured before. Above 40 m, DTS temperatures were lower. Within the interval $40 - 120$ m, temperatures were higher. Below, they were lower, again. For furhter details, see Section 3.2.1.

4 Discussion

4.1 Installation

After the installation, damages to the cable were detected at three positions. Despite the damages, however, temperature measurements could be performed. The following points were identified as possible reasons for the damaging of the cable during installation:

1. **Lithology:** The well is drilled in very young, brittle and unconsolidated rock formations. Rock fragments might have been carried along with the casing during installation which could have damaged the cable in narrow wellbore sections.

2. **Wellbore breakouts:** Large wellbore breakouts occurred within the penetrated rock formations. The cable might have been damaged due to a possible loss of centralization of the casing within these breakout sections.
3. **Movement of centralizers:** After the bottom of the wellbore had been touched, the casing was lifted about 5 m to reach its final position. This might have led to a differential movement between casing and centralizers to which the cable is attached to.

Similar permanent installations of fibre optic cables behind casing have been successfully performed at other sites, e.g. in sedimentary successions at Mallik, Canada (Henninges et al, 2005a), Ketzin, Germany (Prevedel et al, 2008), or the Daqing Oilfield in China (Zhou et al, 2010). Although the length of these installations exceeded the one in Iceland by a factor of 3-4 and the clearance between casing and formation was even smaller at these sites, the cables have been installed without any, or only minor damages. Compared to these installations, the brittle nature of the rock formations seems to be a reasonable explanation for the damages encountered during the installation described herein.

During flow testing and hence warming of the well, further damages were detected. These are attributed to the thermal expansion of the casing.

4.2 Temperature Measurements

First DTS Logging Campaign: Cementation The measured annular temperature changes due to the exothermic hydration of the cement slurry. The period of the observed temperature variations with depth resembles the length of individual casing pipes. The temperature variations along the profile, therefore, correspond to the location of the cable within the annulus. Higher temperatures generally correspond to locations where the cable is fully embedded in cement, lower temperatures correspond to depth sections, where the cable is either attached to the colder casing or little cement is in place.

During the first eight hours, temperature variations are caused by the pumping of cement. The slurry temperature was slightly higher than the well temperature after the drilling process. After pumping, the heat of hydration led to the rapid increase of temperatures along the well axis. The water table within the well was at 107 m after the cement string was removed. Temperatures above, increased to much higher values than below due to the difference in density and specific heat capacity between fluid and air filling the well. This greatly influences the measured temperature profile before filling the casing.

Second DTS Logging Campaign: Flow Test The measured annular temperature depends on the wellbore conditions, i.e. undisturbed or static temperature, bleeding or flow testing conditions. Furthermore, the measured temperature is dependent on the cable-casing distance as well as the cement quality behind the different casings. From the CBL of the production casing it is known, that

the cement bonding is homogeneous over the entire depth interval of DTS measurements. Therefore, effects of different cement qualities behind the production casing on the measured DTS temperatures is assumed to be negligible (Reinsch, 2012).

During static temperature conditions ($0 - 20$ h_{DTS}), temperatures within the annulus were constant except for the uppermost 78 m, where two separate temperature maxima could be observed. These temperature maxima can be explained by two separate aquifers. The upper aquifer is between 0 and 37 m depth, and the lower between 39 and 78 m (Figure 3). Relatively high temperatures of 28 °C might be related to the geothermal surface activity found in a distance of approx. 250 m to the SE (Saemundsson, 1995). Vapour might migrate along permeable layers, i.e. aquifers, within this depth ranges. Furthermore, these layers might have been previously heated during flow testing of the neighbouring well HE-36 and seeping of hot geothermal fluid into the ground.

During bleeding of the well ($20 - 46$ h_{DTS}), gas pressure was released at the wellhead and the water table could rise to the surface. The ascent of fluid from below the cable led to an increase in measured temperatures within the first 10 h of bleeding. When the fluid table reached the wellhead (32 h_{DTS}), the rapid ascent of warmer fluid from deeper parts of the well was stopped as the released volume of fluid per unit time is smaller than the volume of gas released per unit time. The temperature slowly cooled down until the well was opened for flow testing after about 46 h_{DTS}.

Due to the rapid ascent of hot fluid ($46 - 356$ h_{DTS}), the temperature within the well increased. The measured temperature within the annulus was strongly influenced by the distance between cable and casing. Small casing-cable distance resulted in high temperatures, greater distance, lower temperatures. Overall, the temperature measured within the annulus is strongly influenced by the thermal properties of the cement in different depth intervals as well as the caliper of the well. Small caliper diameters and little cement within the annulus led to a lower DTS temperature, as heat could be transmitted to the formation more effectively. The strong negative temperature excursions in regions 2 and 4 correspond to the position of damages observed.

Third DTS Logging Campaign: Shut-In DTS temperature measurements have been compared to the undisturbed temperature conditions, measured at the beginning of the second logging campaign and a conventional temperature log from the neighbouring well HE-36. Large temperature differences were observed between the assumed undisturbed temperature profile from the second field campaign and measurements from the third campaign. DTS temperatures of −4 °C, as observed after the 8.5 month shut-in period, can be attributed to the degradation of the fibre and do not resemble actual formation temperatures. Furthermore, temperature variations along the profile, e.g. in about 150 m depth can be correlated with large changes in the attenuation profile.

It remains to be mentioned that the DTS temperature profile from before the flow test might not resemble undisturbed formation temperatures. During

drilling activities, the well was actively cooled down. Possibly, the static temperature of the permeable layers at top (above and below 40 m), did not fully recover during the 1 month shut-in period between well completion and beginning of the flow test. Furthermore, changing geothermal activity within the aquifers, an influence of the subsurface leakage in HE-53 or seeping of geothermal fluid into the aquifer during flow testing might be possible explanations for the deviation between the two measurements. From the comparison with temperature data of well HE-36, however, undisturbed formation temperatures can be assumed for the depth interval 120-150 m.

4.3 Attenuation Measurements

Attenuation measurements can help to identify different degradation mechanisms of the optical fibre. At low temperature conditions, only mechanical stress acting on the optical fibre can cause locally increased attenuation values and hence influence the measured DTS temperature. Hydrogen ingression is inhibited by the hermetic carbon coating. At elevated temperatures, however, three degradation mechanisms, leading to a persistent attenuation change along the fibre can be assigned:

1. Mechanical stress onto the cable due to differences in thermal expansion of the subsurface installations during the flow test.
2. Thermal degradation of the coating material due to the exposure to high temperatures.
3. Chemical degradation of the light guiding silica structure due to the cracking of oil within the cable and an increased diffusion rate of molecules within the silica at high temperatures.

The first issue leads to a localized increase in loss values and is strongly dependent on the temperature. A strong increase in the attenuation ratio 1300 nm/850 nm has been observed for this loss mechanism (see below). The second issues would result in a smooth overall increase in attenuation at all wavelengths. Loss increase caused by microbending is commonly not wavelength dependent (Buck, 2004). Chemical degradation is most probably caused by the ingression of hydrogen, released from the cable itself (Reinsch, 2012). As the inner stainless steel loose tube was not filled with gel, a migration of hydrogen along the fibre is possible. It should be observed, therefore, by a smooth increase in the differential loss between 1300 nm and 850 nm along the entire fibre.

First DTS Logging Campaign: Cementation During the installation, the cable was accidentally cut two times in 179.6 m on the western branch and 261.2 m on the eastern branch. Furthermore, the local attenuation increase in 235 m on the eastern branch indicates a mechanical damage. As only single ended measurements could be performed and bending loss can be wavelength dependent, absolute temperature readings from below this damage are skewed. Reliable

temperature information, therefore was recovered down to 179.6 m and 235 m, respectively.

Second DTS Logging Campaign: Flow Test Different mechanisms of degradation could be assigned to different regions (Figure 5(a)). Whereas only little changes were observed in region 1, significant changes were observed for the other regions. The strong increase of the attenuation ratio with temperature during the onset of the flow test indicates mechanical stress onto the fibre (region 2). Due to the thermal expansion of the subsurface installations, the cable and thus the fibre became either squeezed in a certain depth range or bending occurred in this depth. Due to a further increase in temperature during the flow test, the attenuation ratio continues to increase as well. Beside mechanical stress, an increased hydrogen load of the fibre might partly attribute to the change in the attenuation ratio 1300 nm/850 nm. Only chemical stress alone, however, cannot account for the strong attenuation increase. If the temperature increase lead to an increase in the hydrogen load alone, this should have been observed in depth intervals with similar temperatures, as well.

During the flow test, temperature rose quickly over the entire length of the cable. With increasing temperature, the intensity of elastically backscattered photons (Rayleigh scattering) increases, increasing the overall loss along the cable. The absolute attenuation at 850 nm remained at a similar value in region 1 between the end of the first logging campaign (2.3 dB/km) and the beginning of the flow test (2.4 db/km). The increase at the end of the second logging campaign (2.7 dB/km) can be partly attributed to an increased Rayleigh scattering intensity with increasing temperature. The relative temperature sensitivity of the Rayleigh signal is approximately $0.005 - 0.008\ \%/°\mathrm{C}$ (Grattan and Meggitt, 1995; Ikushima et al, 2000). For a temperature increase along the fibre of 200 °C, the relative increase in attenuation is $1 - 1.6\ \%$, whereas 13 % have been observed. On the one hand, this difference might be explained by the fact that the relative attenuation increase with temperature is just an approximate value. No reference measurements with this fibre type have been performed. On the other hand, the increased attenuation might be attributed to an increased thermal degradation of the fibre. The latter explanation is more probable, as the difference between calculated and observed changes is in the order of one magnitude and the attenuation continuously increased during the measurement. As the attenuation is continuously increasing at elevated temperatures, the change in attenuation can be regarded as irreversible (Reinsch and Henninges, 2010).

As described in Reinsch and Henninges (2010), irreversible attenuation changes in polyimide fibres are caused by curing, thermal, thermo-oxidative and moisture-induced degradation at elevated temperatures (Cella, 1996; Stolov et al, 2008). The coating material looses plasticity and mechanical stress onto the silica increases irreversibly. A subsequent change in temperature, like cooling the fibre, would lead to a reversible attenuation change due to the different coefficients of thermal expansion between the degraded coating and the silica.

Region 3 shows a small, but gradual increase of the attenuation ratio over time. This indicates chemical changes to the fibre, changing the optical transmission properties. Although the exact mechanism of the degradation process cannot be determined with the available data alone, hydrogen ingression and the subsequent formation of hydroxyl within the fibre is a probable scenario. The increased degradation can be observed by the strong increase of the attenuation at 850 nm, as well (Figure 5(a), profiles 0 and 356 h_{DTS}). With reference to region 1, the attenuation increase due to thermal degradation of the coating material should be lower than observed.

Below region 3, attenuation increases with depth until the cable was cut in 235 m, the position of the previously identified damage from the installation. What led to the increased attenuation slightly above this depth cannot be determined from the available data.

Third DTS Logging Campaign: Shut-In A mechanical damage of the cable occurred in region 2 at approx. 175 m depth. The steep overall attenuation profile in region 1 at wavelengths distant to the typical hydroxyl absorption bands, might be caused by a thermal degradation of the coating material. As the attenuation is strongly correlated to the temperatures experienced during the flow test, the fibre coating shows a different degree of thermal degradation and thus a different increase in microbending loss. Following the results of Reinsch and Henninges (2010), the high attenuation increase can both be attributed to a reversible and an irreversible attenuation increase. For a measurement at higher temperatures, therefore, the overall attenuation would most probably be lower than the observed 18.9 dB/km.

The increase in the attenuation ratio 1300 nm/850 nm indicates an increase in the hydrogen load of the fibre (Figure 6(a), region 1, 9047 h_{DTS}). As the cable could not be flushed with inert gas, the ingression of hydrogen into the fibre from the cable itself could not be reduced. Due to the ingression of hydrogen, the attenuation ratio between the Stokes and the Anti-Stokes band changed in the course of the flow test. This, most likely led to the skewed temperature profile which was measured in August 2010. During the second logging campaign, however, such a severe degradation of the temperature signal was not observed.

4.4 Accuracy

First DTS logging campaign: Cementation Although, relative temperature readings are quite accurate, the absolute accuracy is difficult to determine due to the absence of a reference temperature point along the cable.

To validate the absolute temperature accuracy, temperature data from the SEL has been compared to temperature data from the Hellisheiði weather station. The distance to the weather station is approx. 1.5 km to the north east. In between weather station and well, a flat topography predominates and

the elevation above the sea level is similar to the elevation of the well. Absolute temperature differences can mainly be influenced by different factors:

1. Erroneous temperature readings of the DTS system.
2. Erroneous temperature readings of the weather station.
3. Microclimatic temperature differences caused by the rig itself or the topography between the weather station and the well.

The first aspect seems to be the most important factor for the constant temperature offset, as only single ended measurements could be performed. Small variations are caused by microclimatic temperature changes due to the heat produced by the rig itself. Smaller temperature differences at lower wind speeds, i.e. higher temperatures measured at the SEL, correspond to a longer residence time of the wind above the rig, before it reached the SEL.

A degradation of the optical fibre has not been detected. Therefore ΔT_{deg} is assumed to be 0.

Second DTS logging campaign: Flow Test Temperature measurements within and below region 2 are influenced by mechanical stress onto the fibre. Therefore, only region 1 is considered in the following.

A degradation of the temperature accuracy caused by a wavelength dependent attenuation change and an increased attenuation ratio has not been observed in Figure 6(a), although the attenuation at 850 nm slightly changed. Therefore, a degradation of the temperature accuracy based on a wavelength dependent attenuation change could not be detected (ΔT_{deg} =0 °C).

A possibility to access information about the accuracy is the temperature evolution at the wellhead compared to the temperature evolution in a hot section of the cable (Figure 4). For the later period of logging ($200 - 340$ h_{DTS}), the wellhead temperature increase is similar to the DTS temperature increase. Both temperature evolutions have been linearly fitted. The temperature increase for the wellhead temperature was 0.1120 °C/h, whereas for the cable it was slightly different 0.1179 °C/h. For a flow testing period of 300 h, this results in a temperature difference of ΔT_{slope} =1.77 °C.

The difference indicates a non-constant temperature difference between both measurements, which was expected as heat is constantly transferred to the formation. It has to be noted, that the wellhead temperature has not been measured in the same depth as the DTS temperature used for this comparison. Temperature trends within the well might be slightly different than at the wellhead. In region 1, an increased measurement error could therefore not determined using this temperature comparison.

Bad connectors increase the differential attenuation and have an influence on the calculated temperatures. The error of a DTS temperature measurement, introduced by a bad connector ΔT_{con}, has been determined to be up to 2.0 °C. For a damaged fibre optic extension, the increased differential attenuation resulted in an error of 4.6 °C.

Accounting for the different contributions (calibration, connector, relative accuracy, degradation) and neglecting the error introduced by a damaged fibre

optic extension, the absolute error within region 1 has been estimated to be $\Delta T_{DTS} = 2.6$ °C. As no reference temperature measurements are available for the flow testing period, the error cannot be determined directly. A wellbore temperature simulation (e.g. Francke and Saadat, 2012), however, might help to narrow the error estimate. As the uncertainty of some of the necessary parameters for such a calculation is considerable, the benefit is questionable. Therefore this has not been performed within this study.

In the low temperature range, measured temperatures are more accurate, as the influence of a bad connector is smaller. The absolute deviation for the uppermost part of the fibre (i.e. close to the wellhead) is probably better than 1 °C, which can be validated with ice bath measurements.

Third DTS logging campaign: Shut-In The strong degradation of the optical fibre lead to an increased measurement error of $\Delta T_{deg} > 10$ °C.

5 Conclusions and Outlook

Within this study, a novel fibre optic cable has been developed and tested under field conditions in a high temperature geothermal well in the Hellisheiði geothermal field, SW Iceland. As sensing element, a polyimide fibre with an additional carbon coating has been used. The cable has been installed permanently behind the anchor casing of well HE-53 to 261.3 m depth and the temperature evolution during cementing and flow testing of the well was monitored. Maximum temperatures of up to 230 °C were measured during the onset of the flow test with an accuracy of 2.6 °C.

During the installation, the cable has been damaged at several positions. A loop configuration with a 180° spacing of the cable branches proved to be successful in enabling measurements over the complete installation length despite the encountered damages. The damages can be attributed to the properties of the young and brittle igneous rock formations and individual operational details during running of the casing. For future installations in comparable lithologies, the mechanical properties of the cable and the protection during installation has to be improved. A more protective modification of the bottom centralizer has to be developed to prevent a damage at the turnaround of the cable. Furthermore, pulling back of the casing should be avoided if the casing is carrying instrumentation. Increasing the number of wiper trips prior to the installation of an instrumented casing might be a further possible measure to reduce the number of loose rock fragments in unconsolidated and brittle formations similar to those occurring in Iceland.

Using OTDR measurements at 850 and 1300 nm, different influences on the measurement performance could be detected during the flow test. Attenuation values at 850 nm as well as the attenuation ratio 1300/850 nm were successfully used to distinguish different degradation effects along the cable. Not only mechanical damages to the cable, but also chemical changes to the

fibre as well as thermal degradation of the coating material at high temperatures could be assigned to different regions along the fibre. As the cable was damaged during the installation, flushing the cable continuously with Argon was not possible. Therefore the concentration of harmful substances like hydrogen, most likely produced within the cable itself at elevated temperatures could not be reduced. Flushing the cable, however, would have greatly reduced the chemical and thermal degradation of the fibre.

After the end of the two-week logging campaign, wellhead temperatures reached more than 280 °C, which exceeded the maximum temperatures expected for this well and approached the maximum temperature stability of the optical fibre when heated in an oxygen containing environment. As flushing of the cable was not possible, the temperature profile during the third field campaign after the end of the flow test was significantly affected by the degradation of the optical fibre. Beside erroneous temperature readings, the strong attenuation limits the accessible length if the cable was installed along the entire wellbore. With an optical budget of 20 dB for most commercially available DTS systems, a length of about 1 km could be accessed if the attenuation reached 20 dB at 1064 nm.

Using temperature data, acquired during the first logging campaign, the performance of the cement emplacement during the installation of the anchor casing will be evaluated. Data from the flow testing period will be used to examine the thermal stress on the subsurface installation during rapid temperature changes.

Acknowledgements This work was performed within the framework of the HITI project (http://www.hiti-fp6.eu/), funded by the European Commission in the 6th Framework Programme, Proposal/Contract no.: 019913 and the GeoEn (Phase 2) project and funded by the Federal Ministry of Education and Research (BMBF, 03G0767A). The authors would like to thank J. Schrötter, C. Cunow and M. Poser for their help during planning, installation and data acqusition as well as nkt cables GmbH for the cooperation in developing of a new cable design and providing a cable. Furthermore, the authors are grateful to Sigvaldi Thordarson and the staff from ISOR (Iceland GeoSurvey) for the coordination of the field work and the support during the measurement campaigns, Reykjavik Energy for providing a well for installation as well as Mannvit and Iceland Drilling for the support during installation and measurements.

References

Albertsson A, Bjarnason JO, Gunnarsson T, Ballazus C, Ingason K (2003) Part III: Fluid Handling and Evaluation. In: Fridleifsson GO (ed) Iceland Deep Drilling Project, Feasibility Report, Orkustofnun Report OS-2003-007, p 33

Aminossadati SM, Mohammed NM, Shemshad J (2010) Distributed temperature measurements using optical fibre technology in an underground mine environment. Tunnelling and Underground Space Technology 25(3):220 – 229, DOI 10.1016/j.tust.2009.11.006, URL http://www.sciencedirect.com/science/article/pii/S0886779809001205

Arnórsson S (1995) Geothermal systems in Iceland; structure and conceptual models; I, High-temperature areas. Geothermics 24:561–602, DOI 10.1016/0375-6505(95)00025-9

Bignall G (2010) Hotter and deeper: New zealand's research programme to harness its deep geothermal resources. In: Proceedings World Geothermal Congress 2010, Bali, Indonesia

Buck JA (2004) Fundamentals of Optical Fibers. Wiley Series in Pure and Applied Optics, John Wiley & Sons, Inc.

Cella JA (1996) Degradation and stability of polyimides. In: Ghosh MK, Mittal KL (eds) Polyimides: fundamentals and applications, Marcel Dekker, Inc., New York, pp 343–366

Dowdle W, Cobb W (1975) Static formation temperature from well logs - an empirical method. Journal of Petroleum Technology 27(11):1326–1330, DOI 10.2118/5036-PA

Driesner T, Heinrich CA (2007) The system H2O-NaCl. Part I: Correlation formulae for phase relations in temperature-pressure-composition space from 0 to 1000ă°C, 0 to 5000ăbar, and 0 to 1 XNaCl. Geochimica et Cosmochimica Acta 71(20):4880–4901, DOI 10.1016/j.gca.2006.01.033

Förster A, Schrötter J, Merriam DF, Blackwell DD (1997) Application of optical-fiber temperature logging—an example in a sedimentary environment. Geophysics 62(4):1107–1113, DOI 10.1190/1.1444211

Francke H, Saadat A (2012) Thermal-hydraulic measurements and modelling of the brine circuit in a geothermal doublet. Environmental Earth Sciences This issue

Franzson H, Kristjánsson BR, Gunnarsson G, Björnsson G, Hjartarson A, Steingrímsson B, Gunnlaugsson E, Gíslason G (2005) The Hengill-Hellisheiði geothermal field. Development of a conceptual geothermal model. In: Proceedings World Geothermal Congress 2005, Antalya, Turkey

Freifeld BM, Finsterle S, Onstott TC, Toole P, Pratt LM (2008) Ground surface temperature reconstructions: Using in situ estimates for thermal conductivity acquired with a fiber-optic distributed thermal perturbation sensor. Geophysical Research Letters 35(14):L14,309

Fridleifsson GO, Elders WA (2005) The Iceland Deep Drilling Project: a search for deep unconventional geothermal resources. Geothermics 34:269–285, DOI 10.1016/j.geothermics.2004.11.004

Geckeis O, Nolden W, Henninges J, Zimmer M, Reinsch T (2011) Verfahren zum Betreiben eines Bohrlochkabels und Bohrlochkabel. German Patent DE102008026082B8

van de Giesen N, Steele-Dunne SC, Jansen J, Hoes O, Hausner MB, Tyler S, Selker J (2012) Double-ended calibration of fiber-optic raman spectra distributed temperature sensing data. Sensors 12(5):5471–5485, DOI 10.3390/s120505471

Günzel U, Wilhelm H (2000) Estimation of the in-situ thermal resistance of a borehole using the distributed temperature sensing (DTS) technique and the temperature recovery method (TRM). Geothermics 29(6):689–700, DOI 10.1016/S0375-6505(00)00028-6

Grattan KTV, Meggitt BT (1995) Optical Fiber Sensor Technology. Chapman & Hall, London

Hartog A (1983) A distributed temperature sensor based on liquid-core optical fibers. Journal of Lightwave Technology 1(3):498–509, DOI 10.1109/JLT.1983.1072146

Henninges J (2005) Thermal properties of gas-hydrate-bearing sediments and effects of phase transitions on the transport of heat deduced from temperature logging at mallik, nwt, canada. PhD thesis, Technical University Berlin

Henninges J, Huenges E, Burkhardt H (2005a) In situ thermal conductivity of gas-hydrate-bearing sediments of the Mallik 5L-38 well. Journal of Geophysical Research (Solid Earth) 110:B11,206, DOI http://dx.doi.org/10.1029/2005JB003734

Henninges J, Zimmermann G, Büttner G, Schrötter J, Erbas K, Huenges E (2005b) Wireline distributed temperature measurements and permanent installations behind casing. In: World Geothermal Congress, Antalya, Turkey

Humbach O, Fabian H, Grzesik U, Haken U, Heitmann W (1996) Analysis of oh absorption bands in synthetic silica. Journal of Non-Crystalline Solids 203:19 – 26, DOI 10.1016/0022-3093(96)00329-8

Hurtig E, Grosswig S, Jobmann M, Kuhn K, Marschall P (1994) Fiber-optic temperature measurements in shallow boreholes: experimental application for fluid logging. Geothermics 23(4):355–364, DOI 10.1016/0375-6505(94)90030-2

Ikushima AJ, Fujiwara T, Saito K (2000) Silica glass: A material for photonics. Journal of Applied Physics 88(3):1201–1213, DOI 10.1063/1.373805

Johnson D, Sugianto R, Mock P, Jones C (2004) Identification of steam-breakthrough intervals with DTS technology. SPE Production & Facilities 19:41–48, DOI 10.2118/87631-PA

Kaura J, Sierra J (2008) High-temperature fibers provide continuous DTS data in a harsh SAGD environment. World Oil and Gas Journal 229(6):47–53

Lee CE (2007) Self-calibrating technique enables long-distance temperature sensing. LaserFocusWorld 43(8)

Lemaire PJ, Lindholm EA (2007) Hermetic optical fibers: Carbon-coated fibers. In: Méndez A, Morse TF (eds) Specialty Optical Fibers Handbook, Academic Press, chap 14, pp 453–490

Lemmon EW, Huber ML, McLinden MO (2007) NIST Standard Reference Database 23: Reference Fluid Thermodynamic and Transport Properties-REFPROP, Version 8.0. National Institute of Standards and Technology, Gaithersburg

Lingle, Jr R, Peckham DW, McCurdy A, Kim J (2007) Light-guiding fundamentals and fiber design. In: Méndez A, Morse TF (eds) Specialty Optical Fibers Handbook, Academic Press, chap 2, pp 19–68

Níelsson S, Franzson H (2010) Geology and hydrothermal alteration of the Hverahlid HT-system, SW-Iceland. In: Proceedings World Geothermal Congress 2010, Bali, Indonesia

Normann R, Weiss J, Krumhansl J (2001) Development of Fibre Optic Cables for Permanent Geothermal Wellbore Deployment. In: Twenty-Sixth Work-

shop on Geothermal Reservoir Engineering, Stanford University, Stanford, California

Nowak T (1953) The estimation of water injection profiles from temperature surveys. Petroleum Transactions, AIME 198:203–212

Pimenov V, Brown G, Tertychnyi V, Shandrygi A, Popov Y (2005) Injectivity profiling in horizontal wells via distributed temperature monitoring. In: SPE Annual Technical Conference and Exhibition, 9-12 October 2005, Dallas, Texas

Prevedel B, Wohlgemuth L, Henninges J, Krüger K, Norden B, Förster A, the CO2SINK Drilling Group (2008) The CO2SINK boreholes for geological storage testing. Scientific Drilling 6(6):32–37, DOI doi:10.2204/iodp.sd.6.04.2008

Reinsch T (2012) Structural integrity monitoring in a hot geothermal well using fibre optic distributed temperature sensing. PhD thesis, Clausthal University of Technology

Reinsch T, Henninges J (2010) Temperature-dependent characterization of optical fibres for distributed temperature sensing in hot geothermal wells. Measurement Science and Technology 21(9):094,022, DOI 10.1088/0957-0233/21/9/094022

Reinsch T, Henninges J (2012) Fibre optic distributed temperature sensing - data from geothermal well HE-53, Hellisheidi geothermal field, SW Iceland. Tech. Rep. STR 1212, Helmholtz Centre Potsdam German Research Centre for Geosciences, DOI 10.2312/GFZ.b103-12128

Saadat A, Frick S, Kranz S, Regenspurg S (2010) Energetic use of EGS reservoirs. In: Huenges E (ed) Geothermal Energy System - Exploration, Development, and Utilization, John Wiley & Sons, Ltd., chap 6, pp 303–372

Saemundsson K (1995) Hengill, geological map (bedrock) 1:50000. Orkustofnun, Hitaveita Reykjavíkur and Landmaelingar Íslands

Sigfusson B, Gunnarsson I (2011) Scaling prevention experiments in the hellisheiði power plant, iceland. In: Proceedings, Thirty-Sixth Workshop on Geothermal Reservoir Engineering, Stanford University, Stanford, California, SGP-TR-191

Sims R, Schock R, Adegbululgbe A, Fenhann J, Konstantinaviciute I, Moomaw W, Nimir H, Schlamadinger B, Torres-Martínez J, Turner C, Uchiyama Y, Vuori S, Wamukonya N, Zhang X (2007) Energy supply. In: Metz B, Davidson OR, Bosch PR, Dave R, Meyer LA (eds) Climate Change 2007: Mitigation. Contribution of Working Group III to the Fourth Assessment Report of the Intergovernmental Panel on Climate Change, Cambridge University Press, Cambridge, United Kingdom and New York, NY, USA, pp 251–322

Smithpeter C, Normann R, Krumhansl J, Benoit D, Thompson S (1999) Evaluation of a distributed fiber-optic temperature sensor for logging wellbore temperature at the beowawe and dixie valley geothermal fields. In: Twenty-Fourth Workshop on Geothermal Reservoir Engineering, Stanford University, Stanford, California

Stefánsson V, Steingrímsson B (1980) Geothermal logging I - an introduction to techniques and interpretation. Tech. Rep. OS80017/JHD09, Orkustofnun

Stolov AA, Simoff DA, Li J (2008) Thermal stability of specialty optical fibers. Journal of Lightwave Technology 26(20):3443–3451, DOI 10.1109/JLT.2008.925698

Stone J, Walrafen GE (1982) Overtone vibrations of OH groups in fused silica optical fibers. The Journal of Chemical Physics 76(4):1712–1722, DOI 10.1063/1.443210

Suh K, Lee C (2008) Auto-correction method for differential attenuation in a fiber-optic distributed-temperature sensor. Optical Letters 33(16):1845–1847

Tanimola F, Hill D (2009) Distributed fibre optic sensors for pipeline protection. Journal of Natural Gas Science and Engineering 1(4Ű5):134 – 143, DOI 10.1016/j.jngse.2009.08.002

Thorhallsson S (2003) Geothermal well operation and maintenance. In: IGC2003 Short Course, Geothermal Training Programme, The United Nations University, Iceland, Grensásvegur 9, IS-108 Reykjavík, Iceland, pp 195–217, URL http://www.os.is/gogn/flytja/JHS-Skjol/IGC2003ShortCourse/13Sverrir.pdf

Thorhallsson S (2008) Geothermal drilling and well pumps. In: Workshop for Decision Makers on Direct Heating Use of Geothermal Resources in Asia, Geothermal Training Programme, The United Nations University, Iceland, pp 11–18, URL http://www.os.is/gogn/unu-gtp-sc/UNU-GTP-SC-06-42.pdf

Williams GR, Brown G, Hawthorne W, Hartog AH, Waite PC (2000) Distributed temperature sensing (DTS) to characterize the performance of producing oil wells. In: Wang A, Udd E (eds) Proceedings of SPIE, SPIE, vol 4202, pp 39–54, DOI 10.1117/12.411726

Zhou Z, He J, Huang M, He J, Chen G (2010) Casing pipe damage detection with optical fiber sensors: A case study in oilwell constructions. Advances in Civil Engineering 2010:9, DOI 10.1155/2010/638967